Journal of Metals, Materials and Minerals, Vol. 32, No. 4, pp. 118-127, 2022

Optimized parameter of dissimilar joining between Al6061-T6 and height-strength steel with friction stir spot welding process (FSSW)

Anusak SILACHAI[1], and Suriya PRASOMTHONG[2,*]

[1] *Department of Industrial Engineering, Faculty of Industrial Education, Rajamangala University of Technology Suvarnabhumi, 45000, Thailand*
[2] *Department of Industrial Technology, Faculty of Industrial Technology, Nakhon Phanom, 48000, Thailand*

***Corresponding author e-mail:** Suriya.p@npu.ac.th

Received date:
15 September 2022
Revised date
25 October 2022
Accepted date:
2 November 2022

Keywords:
Optimized parameter;
Dissimilar joining;
Friction stir spot welding

Abstract

High-strength steel and aluminum alloys are used to manufacture modern vehicles. The objective was to reduce the weight and fuel consumption of the vehicles. In this study the optimum parameters for the friction stir spot welding (FSSW) process between Al6061-T6 aluminum alloy and HSS590 high-strength steel were determined. Response surface methodology based on central composite design (CCD) with three parameters, five levels, and 19 runs was used to conduct experiments and develop mathematical regression models. The three joint parameters were tool speed, welding feed, and dwell time. Analysis of variance was then performed to examine the adequacy of the developed models. Finally, the effects of the process parameters on the mechanical properties were investigated using mathematical models. In addition, the distribution of the chemical composition and fracture characteristics of the joints was examined using scanning electron microscopy (SEM). The investigation found that the optimum welding parameters were a tool speed of 1576 rpm, welding feed rate of 45 mm·min^{-1}, and dwell time of 10 s. Furthermore, the results confirmed that the mathematical models and experiments were consistent.

1. Introduction

Currently, the most popular materials used in modern automotive manufacturing are aluminum alloys and high-strength steel. Aluminum used in the automotive industry is Al6061-T6 aluminum alloy owing to its high strength and lightweight. [1,2] Both aluminum and steel materials are produced using the required automotive components and are assembled by welding [3]. The most popular welding process in the automotive industry is resistant spot arc welding (RSW), a fusion welding (FW) process suitable for similar welding joints but not dissimilar welding joints. In particular, carbon steel and aluminum [4] have dissimilar physical properties such as melting point temperature (1560°C for steel and 630°C for aluminum alloy), conductivity, and convection. Consequently, the joining of both materials between aluminum and carbon steel by the fusion welding process was unsuccessful. In addition, intermetallic compounds (IMCs) were found in the solidification process between iron and aluminum ($FeAl_2$, Fe_2Al_5, and $FeAl_3/Fe_xAl_x$) [5] with high hardness. Consequently, the ductility is reduced, resulting in a low shear strength of the weld line, which is insufficient for use in engineering structures. Therefore, welding processes that prevent melting must be studied to prevent the formation of intermetallic compounds in the material. According to previous reports, the non-melting welding process used in the welding industry is known as non-fusion welding. Friction welding (FW), friction stir welding (FSW), and friction stir spot welding (FSSW), are processes designed for joining dissimilar welding materials. This method uses mechanical energy to stir mixed materials without melting, causing the materials to be stirred together in a solid state. In addition, the joining was found to be sufficiently strong for dissimilar welding materials [6-9].

Currently, a wide variety of studies have proposed guidelines for experimental design to predict and determine optimal parameters. For example, Nakovong *et al*. [10] studied the optimization of the production factor in FSW welding using Taguchi and ANOVA for tensile strength and weld hardness analysis. Zamani *et al*. [11] joined an Al-SiC aluminum alloy with the FSW process using the response surface method (RSM) to optimize the weld parameters. MohammadiSefat *et al.* [12] experimentally welded aluminum alloy Al5052-H18 using the FSW process. Experimental design using RSM to determine optimum welding parameters. Naqibi *et al.* [13] studied the factors of welding copper-aluminum tubes using the FSW process to determine the optimum value of the Box–Behnken design factor using the RSM method. Kumar *et al*. [14] performed an experimental dissimilar welding joint between Al5083-O and Al6082-T6 with tailor-welded blanks to determine the parameters of FSW welding using the RSM method. Chakradhar *et al*. [15] experimentally joined of aluminum alloy Al6061 using the FSW process to determine the optimal parameters for tensile strength and weld hardness using the RSM method. Mirabzadeh *et al.* [16] examined the heat generated by FSW welding of polypropylene specimens for

process parameter analysis using the RSM (Box-Behnken) method. Ahmadnia *et al.* [17] studied the effect of FSW on the tensile strength, hardness, and elongation of the aluminum weld between Al6061 and Al5051 using the RSM method. Many additional cases of experimental design for predicting and optimizing FSW welding have also been mentioned. From the research mentioned in the paragraph, it is evident that the experimental design can be effectively predicted to find the appropriate value in the research.

As mentioned, friction stir spot welding (FSSW) in the joining of dissimilar welding between Al6061-T6 aluminum alloy and HSS590 high-strength steel was not mentioned. In addition, there have been studies on process adjustments and the various responses to the process. Therefore, this research aims to design a statistical experiment and application of response surface methodology (RSM) using the central composite design quadratic model (CCD). Furthermore, the optimum welding parameters such as tool speeds, feeds, and dwell time affect the tensile load, hardness, and weld elongation. Finally, researchers hope that the CCD method can effectively design the FSSW process and benefit manufacturers and those interested in further study of the FSSW process.

2. Experimental

2.1 Experimental and tensile test

In the investigation of FSSW, the welding parameters of the experiment were tool speed, welding feed, and dwell time in the joint. The CNC machining center (ACCUWAY UL-15) is an experimental machine that can control welding parameters. Welding using plunging is 1.20 mm. A cylindrical welding tool with a diameter of 10 mm, a tool pin diameter of 4 mm, and a 1.20 mm, pin length. Figure 1(a) shows a welding and clamping process explicitly designed for FSSW.

The experiment involved placing an aluminum lab joint on HSS590 steel of 30 mm. as shown in Figure 1(b). The tensile test (model: WAW - 1000D Electro-hydraulic Servo Control Universal Testing machine) and joint hardness are shown in Figures 1(b-c), Therefrom the tensile load, elongation, and hardness to analyze the efficiency of the process which will be discussed in the next section.

2.2 Experimental materials

The experiment used a dissimilar material between Al6061-T6 aluminum alloy and HSS590 high-strength steel. Cutting was 100 mm. with a length and width of 25 mm, and thickness of 1 mm. as shown in Figure 1. In the previous welding process, the workpiece surface was polished with emery paper. In addition, the surface was cleaned with acetone before welding. Table 1 lists the chemical compositions and mechanical properties of the experimental materials.

$$Y = \beta_0 + \beta_1(X_1) + \beta_2(X_2) + \beta_3(X_3) + \beta_{11}(X_1^2) + \beta_{22}(X_2^2) + \beta_{12}(X_1X_2) + \beta_{13}(X_1X_3) + \beta_{23}(X_2X_3) \quad (1)$$

2.3 Experimental design

They determined the optimum factors for welding joint tensile strength, elongation, and hardness using a central composite design (CCD). Because CCD can generate nonlinear correlations using a small number of runs in several experiments, it is suitable for designing experiments. The factors in the study were the tool speed (S; X_1), feed (f; X_2), and dwell time (t; X_3). The factor level was determined based on relevant research and the limitations of the experimental tool. The levels of the factors were low (-1), medium (0), and high (1), as shown in Table 2. The experiment and design used the Design-Expert and MINITAB 19 statistical software packages. Design-Expert software was used for graphical optimization, in this part of the verification of models, coefficient of determination (R^2) and analysis of variance (ANOVA) were used MINITAB. The response equation is shown in equation (1), where Y is the response, and D is the composite desirability (D), where the result is between 0 to 1. If D is equal to 1, the result has complete a composite desirability.

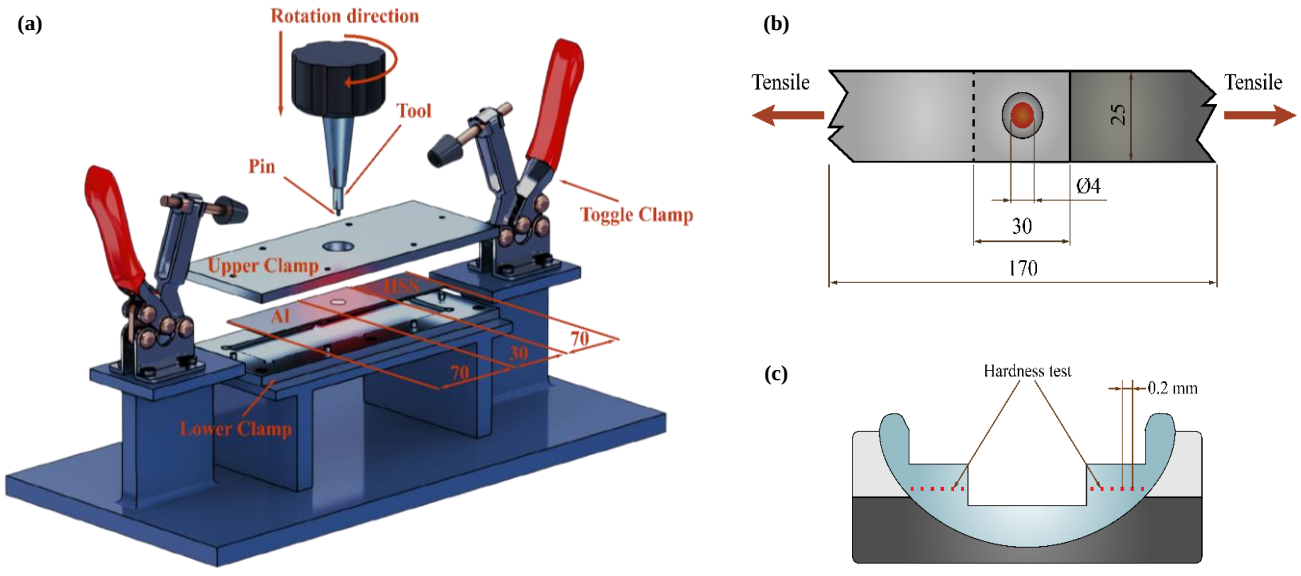

Figure 1. FSSW process, tensile and hardness test of specimen in the experimental.

Table 1. Chemical composition and mechanical properties of the material in the experiment.

Material	Chemical composition								
	Si	**Fe**	**Cu**	**Mn**	**Mg**	**Cr**	**S**	**C**	**Al**
Al6061-T6	0.40	-	0.15	0.00	0.81	0.04	-	0.00	Bal.
HSS590	0.90	Bal.	-	1.25	-	1.45	0.05	0.21	-

Table 2. Factor of experiments along with their levels based on CCD.

Parameters	Level				
	-1.68	**-1**	**0**	**1**	**1.68**
Tool Speed: S (X_1) (rpm)	659	1000	1500	2000	2341
Welding feed: f (X_2) (mm·min^{-1})	6	20	40	60	74
Dwell time: t (X_3) (s)	1.59	5	10	15	18

3. Results and discussion

Table 3 presents the experimental procedure designed with a CCD to study the effects of the parameters on the FSSW process. The results showed that the tensile load were 1.74 KN to 2.58 KN, 1.2% to 16.2% for elongation, and 106 HV to 127.51 HV for hardness. Table 4-6 analyzes the relationship between the response factors for the tensile load (*Ts*), elongation (%*El*), and welded hardness (*HV*).

3.1 Development of response surface models

The response of the process factors related to process quality is determined. A regression analysis developed a mathematical model using the quadratic polynomial method for tensile load, elongation, and weld hardness. In the model development, statistical analysis was used to assess the validity of the full quadratic models by analysis of variance (ANOVA) and coefficient of determination: (R^2). A mathematical model using the polynomial regression method of responses, linear terms, quadratic equations, and interaction terms is demonstrated in Equations (2-4).

$$Ts = 2.53 + 0.0668S + 0.0604f + 0.1416t + 0.0675Sf + 0.0325St + 0.005ft - 0.3692S^2 - 0.1070f^2 - 0.1892t^2 \quad (2)$$

$$El = 13.8 + 1.32S + 0.7822f + 1.15t + 1.11Sf - 0.1312St + 0.2613ft - 3S^2 - 2.23f^2 - 1.32t^2 \quad (3)$$

$$HV = 111.18 + 0.8737S - 1.56f + 3.95t + 0.3188Sf - 0.1312St + 1.15ft + 2.11S^2 + 0.838f^2 + 4.58t^2 \quad (4)$$

Where S is the tool speed, f is the welding feed, and t is the dwell time. *Ts*, *El*, and *HV* are the tensile load, elongation, and weld hardness, respectively.

Table 3. Experimental parameters and results.

Run	Process factors			Process factors		
	Tool speed (rpm)	**Feed (mm·min^{-1})**	**Dwell time (s)**	**Tensile load (KN)**	**Elongation (%)**	**Hardness (HV)**
1	659	40	10	1.52	3.25	113.02
2	1500	74	10	1.95	8.70	113.92
3	1000	60	15	1.87	6.70	118.48
4	2000	60	5	1.94	9.00	108.00
5	2341	40	10	1.93	9.40	122.00
6	1500	40	10	2.56	15.30	106.00
7	1500	40	10	2.55	14.70	108.00
8	1500	40	18	2.53	14.20	131.00
9	1000	60	5	1.75	4.70	113.25
10	1000	20	15	1.86	6.00	127.51
11	2000	20	15	1.84	5.35	120.46
12	1500	6	10	1.95	8.30	113.91
13	1000	20	5	1.65	4.82	116.15
14	1500	40	10	2.58	14.33	114.08
15	1500	40	10	2.45	13.12	113.85
16	1500	40	10	2.4	11.20	113.85
17	1500	40	1.59	2.01	8.00	118.00
18	2000	20	5	1.64	4.92	120.34
19	2000	60	15	2.25	10.70	123.42

Table 4. ANOVA for Quadratic model of *Ts* by RSM.

Source	DF	Adj SS	Adj MS	F-value	p-value
Model	9	2.09	0.2317	18.26	0.0001
S	1	0.1107	0.1107	8.72	0.0161
f	1	0.0492	0.0492	3.88	0.0804
t	1	0.2152	0.2152	16.96	0.0026
Sf	1	0.045	0.045	3.55	0.0923
St	1	0.0041	0.0041	0.3192	0.5859
ft	1	0.0001	0.0001	0.0039	0.9513
S^2	1	1.21	1.21	95.59	0.0001
f^2	1	0.652	0.652	51.38	0.0001
t^2	1	0.1517	0.1517	11.95	0.0072
Residual	9	0.1142	0.0127		
Lack of Fit	5	0.0895	0.0179	2.9	0.162
Pure Error	4	0.0247	0.0062		
Cor Total	18	2.2			

R^2 0.9481, R^2_{adj} 0.8961

Table 5. ANOVA for Quadratic model of El by RSM.

Source	DF	Adj SS	Adj MS	F-value	p-value
Model	9	234.88	26.1	7.27	0.0034
S	1	23.97	23.97	6.67	0.0295
f	1	8.36	8.36	2.33	0.1615
t	1	18.13	18.13	5.05	0.0512
Sf	1	9.79	9.79	2.73	0.1331
St	1	0.1378	0.1378	0.0384	0.849
ft	1	0.546	0.546	0.152	0.7057
S^2	1	123.17	123.17	34.3	0.0002
f^2	1	68.18	68.18	18.98	0.0018
t^2	1	23.63	23.63	6.58	0.0304
Residual	9	32.32	3.59		
Lack of Fit	5	21.78	4.36	1.65	0.3232
Pure Error	4	10.54	2.63		
Cor Total	18	267.21			

R^2 0.8790, R^2_{adj} 0.758

Table 6. The ANOVA results for *HV* by RSM.

Source	Df	Adj SS	Adj MS	F-value	p-value
Model	9	583.72	64.86	3.37	0.0423
S	1	10.43	10.43	0.542	0.4804
f	1	33.2	33.2	1.73	0.2214
t	1	213.47	213.47	11.1	0.0088
Sf	1	0.8128	0.8128	0.0423	0.8417
St	1	0.1378	0.1378	0.0072	0.9344
ft	1	10.51	10.51	0.5464	0.4786
S^2	1	60.72	60.72	3.16	0.1094
f^2	1	9.59	9.59	0.4983	0.4981
t^2	1	286.38	286.38	14.89	0.0039
Residual	9	173.13	19.24		
Lack of Fit	5	113.52	22.7	1.52	0.3522
Pure Error	4	59.61	14.9		
Cor Total	18	756.86			

R^2 0.8790, R^2_{adj} 0.758

An ANOVA was performed to verify the precision of the developed mathematical models, and the results are presented in Table 4. For *Ts* in the table, the model p-value for *Ts* was less than 0.05, indicating that the model conditions were significant. Therefore, the terms *S*, *t*, S^2, f^2, and t^2, which were 0.0161, 0.0026, 0.0001, 0.0001, and 0.0072, respectively, were significant for *Ts*. In contrast, *f*, *Sf*, *St*, and *ft* had P-values higher than 0.05, indicating that the model conditions were insignificant to *Ts*. However, considering "Lack-of-Fit" Table 4, the

p-value is higher than the critical value of 0.162, which is over 0.05, so the null hypothesis is unably rejected. Therefore, it can be concluded that the regression model is suitable such that the equations can be used to predict the *Ts* of the weld. Furthermore, considering that the R^2 value of the model approaches 1, the model can be used to establish predictive equations.

Table 5 is the ANOVA analysis, and the *El* results show that the model p-value for *El* is less than 0.05, indicating that the model conditions are significant. Therefore, the terms *S*, S^2, f^2, and t^2 are 0.0295, 0.0002, 0.0018, and 0.0304, respectively, and are significant for *El*. On the other hand, the other term, a p-value higher than 0.05, indicates that the model conditions were insignificant for *El*. However, considering "Lack-of-Fit" Table 5, the p-value is higher than the critical value of 0.3232, which is over 0.05, so the null hypothesis is unably rejected. Therefore, it was concluded that the regression model is suitable so that the equations can be used to predict *El* of the weld. Furthermore, considering that the R^2 value of the model approaches 1, the model can be used to establish predictive equations.

Table 6. shows the ANOVA analysis, and the *HV* results show that the model of the p-value for the *HV* is less than 0.05, indicating that the model conditions are significant. Therefore, the terms *t* and t^2 are 0.0088 and 0.0039, respectively, and are significant for *HV*. On the other hand, the other term, a p-value higher than 0.05, indicates that the model conditions were insignificant for *HV*. However, considering "Lack-of-Fit" Table 6, the p-value is higher than the critical value of 0.3522, which is over 0.05, so the null hypothesis is unably rejected. Therefore, it was concluded that the regression model is suitable so that the equations could be used to predict the *HV* of the weld. Furthermore, considering that the R^2 value of the model approaches 1, the model can be used to establish predictive equations.

3.2 Optimization and confirmation

This study investigates the joining of Al6061-T6 aluminium alloy with HSS590 steel by the FSSW process on the Ts, El, and HV of welded joints. The optimal parameters are presented in Table 7. The optimal conditions in the experiment were found to be a tool speed of 1576.445 rpm, welding welding feed of 45.09 mm·min^{-1}, and dwell time of 10.08 s. The tensile load is 2.52 KN, 14.2 of the elongation, and 111.10 HV weld hardness. Figure 2 shows the numerical simulation results of the predictive response for the joint between Al6061-T6 aluminum alloy and HSS590 steel using the FSSW welding process, in which the composite desirability was 0.8777.

Therefore, the appropriate values in Table 7 were used. Finally, experiments were repeated to confirm the results. To confirm the experimental results, the researcher parameters were adjusted for the convenience of setting the tool speed to 1576 rpm, welding feed to 45 mm·min^{-1}, and dwell time to 10 s. Then, welding of five additional pieces was performed. Finally, the means of the responses were investigated to confirm the experimental results, as shown in Table 8.

Table 8. The statistical analysis results were verified as confirmation. It was found that the confirmation of the effect for mean *Ts* was 2.34 KN with an error of 7.14%, the mean of *El* was 12.26 and an error of 12.68 %, and the experiment to confirm the effect of the mean *HV* was 105.72 HV has an error of 4.84%. Generally, the experimental results for confirmation were within acceptable limits, with an overall error of no more than 13%.

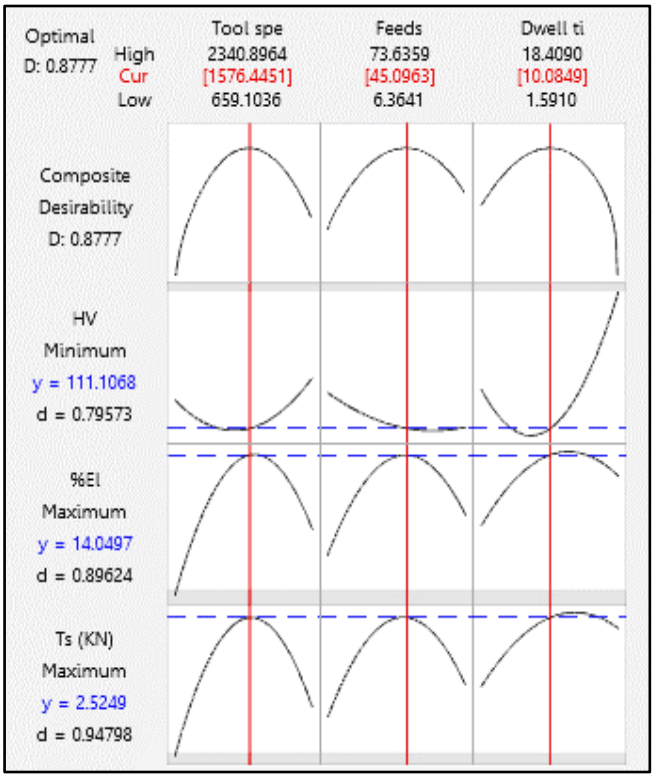

Figure 2. Exhibition of optimal result in FSSW welding on numerical optimization by MINITAB.

Table 7. Optimal results as obtained and response by MINITAB V19 statistical software.

S (rpm)	f (mm·min^{-1})	t (s)	Ts (KN)	El (%)	HV	Desirability (%)
1576.445	45.09	10.08	2.52	14.04	111.10	0.8777

Table 8 The results of the experiments were confirmed with the results of statistical analysis.

Response	Optimization approach	Confirmatory experiment	Error (%)
Ts	2.52	2.34	7.14
El	14.04	12.26	12.68
HV	111.10	105.72	4.84

3.3 Analyzing mechanical properties

The response surface graphs of *Ts*, *El*, and *HV* from equations (Equations 2, 3, and 4) were used for prediction, and then the response surface graph was generated, as shown in Figure 3-5. The perturbation and 3D response surface graphs are shown in Figure 3(a) Effect of the effective parameters (A: tool speed, B: welding feed, C: dwell time) on the *Ts* of the joint. First, the dwell time was observed at the highest *Ts*, followed by the tool speed and welding feed. Figure 3(b-d) show the response surface graphs of the parameter to *Ts* of the joint. The parameter level was in the middle *Ts* of the maximum joint. Conversely, it was found that as the parameter level increased or decreased, *Ts* of the joint decreased. The contour plot showed that the relationship the between process parameter and *Ts* had a nonlinear effect. The middle curve shows the highest *Ts*, and the next curve shows the lowest *Ts* of the joint.

Figure 4 demonstration of the perturbation and 3D response surface graphs. Figure 4(a) exhibits the effect of the effective parameters on the *El* of the joint. Figure 4(b-d) illustrate response surface graphs of parameter on the *El* for the joint. It was found that as the parameter level increased or decreased, *El* of the joint decreased. The contour plot showed the relationship between the process parameter and *El* had a nonlinear effect, The center curve shows the highest *El* and the subsequent curve shows the lowest *El* of the joint.

Figure 5 shows the perturbation and 3D response surface graphs Figure 5(a) The effect of parameters on the *HV* of the joint. Figure 5(b-d) shows the response surface graphs of the parameters to *HV* of the joint. The parameter level was in the middle, illustrating the lowest *HV*. On the other hand, it was found that as the parameter level increased or decreased, the *HV* of the weld increased. The contour plot found that the relationship between the process parameters and *HV* had a nonlinear effect. The center curve shows the lowest *HV*, and the next curve shows the increased *HV* of the joint.

3.4 The chemical and fracture analysis

In the previous section, the efficiency of the FSSW process was investigated using the CCD method. The optimal parameters for the FSSW process were found to be a tool speed of 1576 rpm, welding feed of 45 mm·min^{-1}, and dwell time of 10 s. An examinination of the chemical composition using the EDS-line scan technique is shown in Figure 6. Straight-line investigation from the aluminum side to the steel side. Chemical composition analysis revealed a high aluminium-to-steel dispersion content, as shown in Figure 6(a). Furthermore, an investigation revealed that a line scan of aluminum tilted toward the steel side indicated that aluminum could intermix with steel. Similarly, a line scan of steel with a slope on the aluminum side indicated that the steel interface layer could be stirred with the aluminum. As observed from the chemical composition of the iron at the interface layer, the amount increased. On the other hand, the inappropriate factors for the FSSW process are a tool speed of 660 rpm, welding feed of 73 mm·min^{-1}, and dwell time of 18 s, as shown in Figure 6(b). It was observed that the line scan characteristics of the aluminum slope in steel were less than the optimal factor. This indicates that the interface layer has less adhesion between aluminum and iron. Examination of the chemical composition of the steel at the interface layer revealed that the inappropriate factor was lower than the optimal factor. Because the welding factor is too low for the heating of the interface layer, atomic diffusion does not occur between the two materials. Consequently, the adhesion between the two materials is low, resulting in a decrease in the tensile strength.

Therefore, the fracture surface for a couple of factors were compared using SEM technical analysis, as shown in Figure 7. Damage to specimens obtained from tensile tests on the aluminum side Figure 7(a). Demonstrate the damage characteristics of appropriate welding parameters. Ductile damage was observed, surface fractures appeared as dimples and craters, and small dimples were observed on the damaged surface. These characteristics indicate ductile damage at high tensile load, which is consistent with the results reported by Guishen *et al.* [18]. In addition, the uniformity of the dimples and craters indicated a high amount of plastic deformation. On the other hand, when the parameters were adjusted the tool speed was 660 rpm, welding feed was 73 mm·min^{-1}, and dwell time was 18 s. Therefore, it was an inappropriate parameter for this experiment. Joint damage is a micro-cave with a fracture in a complex plane. This characteristic indicates that brittle damage results in low tensile strength of the joint, as shown in Figure 7(b). The appearance of the micro-cave fracture surface with a plain surface complexion indicates that the damage characteristics have low plastic deformation.

3.5 Disclusion

HSS590 steel and Al6061-T6 aluminium alloy are used in the modern automotive industry. The objectives of reducing weight and fuel consumption include environmental friendliness. Therefore, this study examined the joints of two materials using the FSSW process. In addition CCD mathematical modeling was used to determine the optimal process factor. Investigations have revealed that mathematical models can effectively model predictions [17,19,20]. Therefore, the optimal (S = 1576 rpm, f = 45 mm·min^{-1}, and t = 10 s) and inappropriate (S = 660 rpm, f = 73 mm·min^{-1}, and t = 18 s.) was repeated to confirm the experimental results. In addition, the chemical composition and surface fractures at the interfaces of the coupled specimens were examined. It was found that the samples established by the optimal factor had a higher Fe content at the interface than those established by the inappropriate factor. This indicates that the appropriate weld factor exhibits adhesion in the region of the interface. This indicates that the optimum joint factor is adhesion between Fe and Al in the interface region [5]. Then, considering the fracture surface of these coupled factors, the difference in tensile strength was further demonstrated. This is because the fracture surface characterizes the optimal factor as ductile fracture. On the other hand, an inappropriate welding factor, that is, the fracture surface, is characterized by brittle fracture. Finally, to illustrate the differences between the studies, the authors compared their performance with those of other techniques, as shown in Table 9.

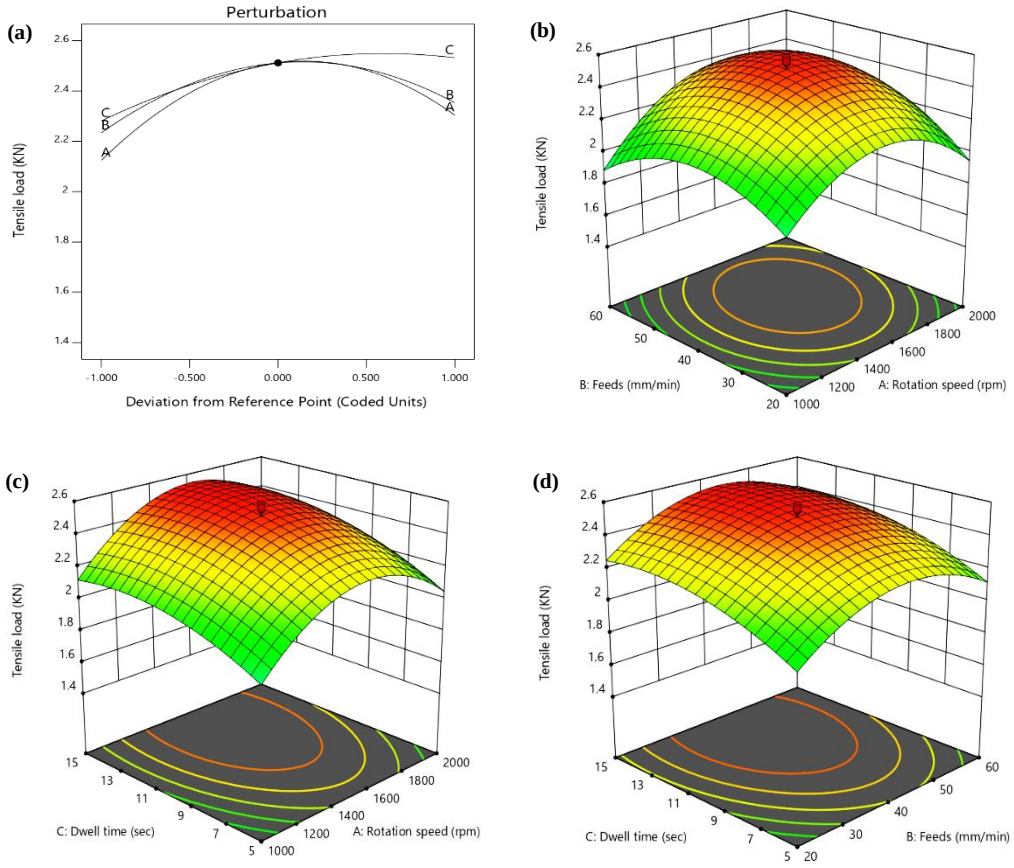

Figure 3. Perturbation and 3D response surface graphs showing the effects of all the factors on *Ts*.

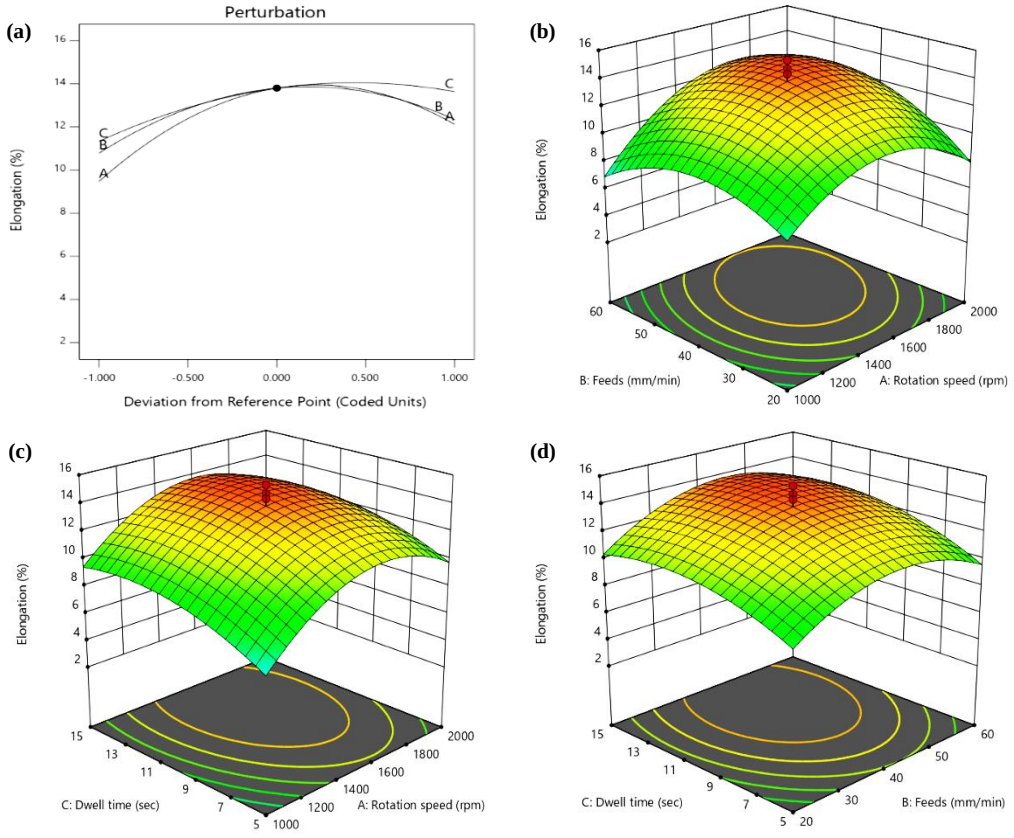

Figure 4. Perturbation and 3D response surface graphs showing the effects of all the factors on the *El*.

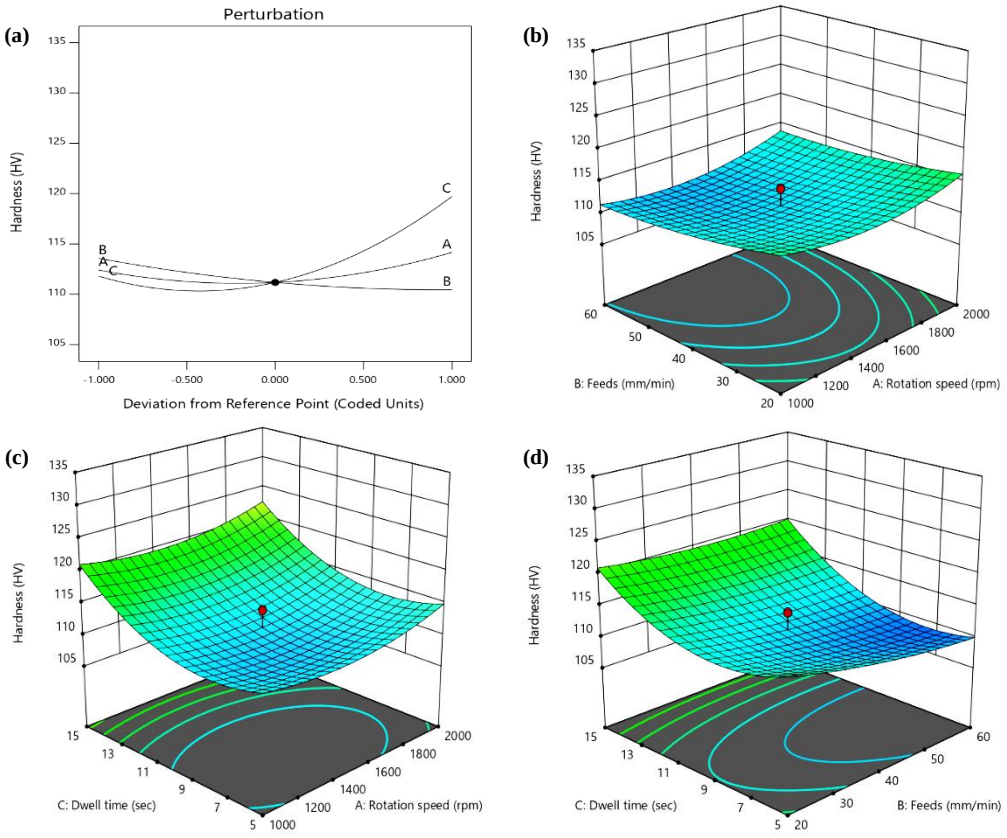

Figure 5. Perturbation and 3D response surface graphs showing the effects of all the factors on the *HV*.

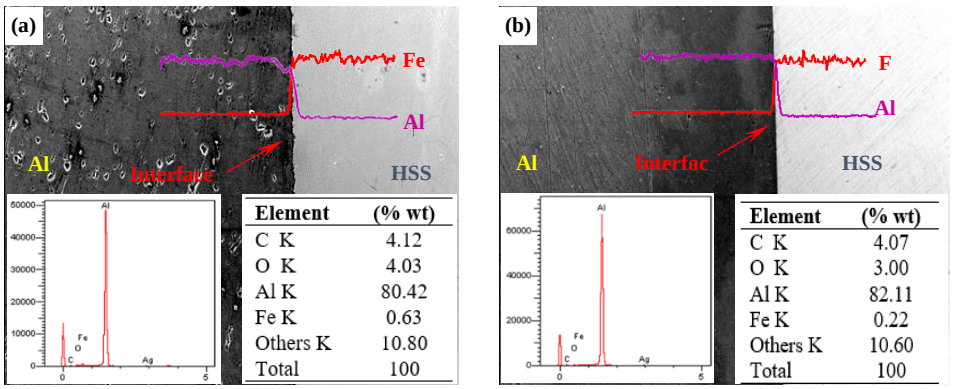

Figure 6. The results of chemical analysis techniques EDS-Line scan (a) tool speed to 1576 rpm, welding feed 45 mm·min^{-1}, and dwell time 10 s, (b) tool speed to 660 rpm, welding feed 73 mm·min^{-1}, and dwell time 18 s.

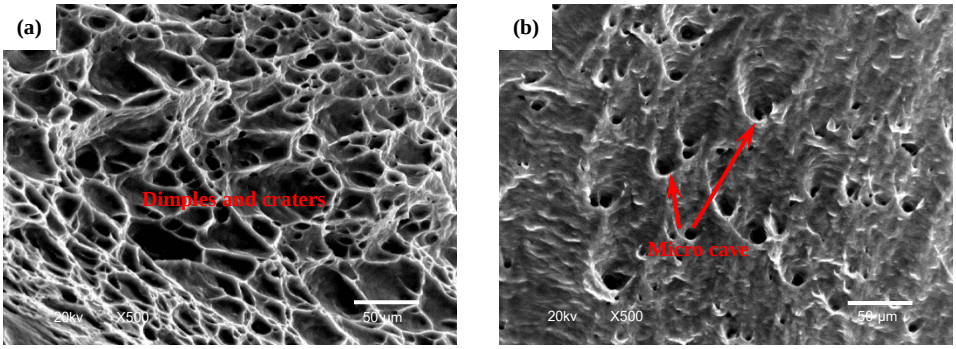

Figure 7. The investigation fracture mechanic of FSSW (a) tool speed to 1576 rpm, welding feed 45 mm·min^{-1}, and dwell time 10 s, (b) tool speed to 660 rpm, welding feed 73 mm·min^{-1}, and dwell time 18 s.

Table 9. Summary of performance and reference research.

Ref.	Method	Material	Tensile load (KN)	Hardness (HV)	% El	Chemical and fracture analysis
[1]	N/A	6111-T4 and steel DC04	3.5	82	N/A	N/A
[2]	Area analysis	Al 6016/IF-steel	1.8/4.5	1000/1100	N/A	Examine
[3]	N/A	boron steel	3.5	280	N/A	N/A
[4]	N/A	DP600	3.5	350	N/A	Examine
[6]	N/A	DP780GA/ TRIP780	13.2 /13.2	442/200	N/A	N/A
[7]	N/A	Al 6061-T4	4.6	N/A	N/A	N/A/ Examine
[8]	N/A	Low carbon steel /Al-Mg alloy	3.0	N/A	N/A	Examine
[9]	N/A	AM60/DP600 steel	1.65/2.07	N/A	N/A	N/A / Examine
This work	CCD	HSS590/Al6061-T6	2.52	111.10	14.04	Examine

4. Conclusions

Optimal parameters of dissimilar material joints between HSS590 high-strength steel and Al6061-T6 aluminium alloy with the FSSW process. The factors examined were tool speed, welding feed and dwell time on mechanical properties such as tensile load, elongation, and joint hardness. RSM mathematical and statistical analyses were applied along with CCD experimental design. The three variables were related to each other using mathematical models for effectively predicting the tensile load, elongation, and joint hardness, with coefficients of determination of 0.9481, 0.8790, and 0.8609, respectively. When determining the optimum factor, the optimal conditions for tensile load, elongation and joint hardness were tool speed of 1576 rpm, welding feed of 45 mm·min^{-1}, and dwell time of 10 s is the optimal solution which causes 2.52 KN for tensile load, 111.10 HV for hardness, and 14.04% for elongation. Therefore, verified the obtained optimal results through a confirmatory experiment, and the findings showed that the proposed approach could predict the optimal solutions with overall error values lower than 13%. Finally, the chemical composition and fracture surfaces at the interface layer were examined, and it was found that the optimum factor had a higher elemental content in the interface layer than the inappropriate weld factor. Subsequently, when considering the fracture surface, it was found that the appropriate welding factor was the fracture surface at the interface layer, as indicated by the dimples and craters. However, the fracture surface of the inappropriate welding factor at the interface layer is characterized by a micro-cave fracture surface with a plain surface complexion, indicating that the damage characteristics are low plastic deformation.

Acknowledgements

This study was supported by the Rajamangala University of Technology Suvarnabhumi fund; the fiscal year 2020 Provides funding to support project research “Influence of variable on mechanical properties and the chemical composition of the friction stir spot welding for dissimilar joint” Sincerely Yours.

References

[1] Y. C. Chen, A. Gholinia, and P. B. Prangnell, “Interface structure and bonding in abrasion circle friction stir spot welding: a novel approach for rapid welding aluminium alloy to steel automotive sheet,” *Materials Chemistry and Physics*, vol. 134, no. 1, pp. 459-463, 2012.

[2] S. Bozzi, A. L. Helbert-Etter, T. Baudin, B. Criqui, and J. G. Kerbiguet, “Intermetallic compounds in Al 6016/IF-steel friction stir spot welds,” *Materials Science and Engineering: A*, vol. 527, no. 16-17, pp. 4505-4509, 2021.

[3] Y. Hovanski, M. L. Santella, and G. J. Grant, “Friction stir spot welding of hot-stamped boron steel,” *Scripta Materialia*, vol. 57, no. 9, pp. 873-876, 2007.

[4] M. I. Khan, M. L. Kuntz, P. Su, A. Gerlich, T. North, and Y. Zhou, “Resistance and friction stir spot welding of DP600: A comparative study,” *Science and Technology of Welding and Joining*, vol. 12, no. 2, pp. 175-182, 2007.

[5] S. Prasomthong, and S. Namkeaw, “The Influence of adding aluminum welding wire on mechanical properties and chemical composition of the welding hardfacing welded low carbon steel by gas tungsten arc welding process,” *The Journal of Industrial Technology*, vol. 15, no. 1, pp. 27-36, 2019.

[6] M. Santella, Y. Hovanski ,and T. Y. Pan, “Friction stir spot welding (FSSW) of advanced high strength steel (AHSS),” *SAE International Journal of Materials and Manufacturing*, vol. 5, no. 2, pp. 382-387, 2012.

[7] Y. Tozaki, Y. Uematsu, and K. Tokaji, “A newly developed tool without probe for friction stir spot welding and its performance,” *Journal of Materials Processing Technology*, vol. 210, no. 6-7, pp. 844-851, 2010.

[8] C. Y. Lee, D. H. Choi, Y. M. Yeon, and S. B. Jung, “Dissimilar friction stir spot welding of low carbon steel and Al-Mg alloy by formation of IMCs,” *Science and Technology of Welding and Joining*, vol. 14, no. 3, pp. 216-220, 2009.

[9] T. Liyanage, J. Kilbourne, A. P. Gerlich, and T. H. North, “Joint formation in dissimilar Al alloy/steel and Mg alloy/steel friction stir spot welds,” *Science and Technology of Welding and Joining*, vol.14, no. 6, pp. 500-508, 2009.

[10] K. Nakowong, and K. Sillapasa, “Optimized parameter for butt joint in friction stir welding of semi-solid aluminum alloy 5083 using taguchi technique,” *Journal of Manufacturing and Materials Processing*, vol. 5, no. 3, pp. 1-21, 2021.

[11] S. M. M. Zamani, K. Behdinan, M. R. Razfar, D. H. Fatmehsari, and J. A. Mohandesi, “Studying the effects of process parameters on the mechanical properties in friction stir welding of Al-SiC composite sheets,” *The International Journal of Advanced Manufacturing Technology*, vol. 113, no. 11, pp. 3629-3641, 2011.

[12] M. MohammadiSefat, H. Ghazanfari, and C. Blais, "Friction stir welding of 5052-H18 aluminum alloy: Modeling and process parameter optimization," *Journal of Materials Engineering and Performance*, vol. 30, no. 3, pp.1838-1850, 2021.

[13] M. F. Naqibi, M. Elyasi, H. J. Aval, and M. J. Mirnia, "Statistical modeling and optimization of two-layer aluminum-copper pipe fabrication by friction stir welding," *Transactions of the Indian Institute of Metals*, vol. 75, no. 3, pp.635-651, 2022.

[14] P. Kumar, and S. Sharma, "Influence of FSW process parameters on formability and mechanical properties of tailor welded blanks AA6082-T6 and AA5083-O using RSM with GRA-PCA approach," *Transactions of the Indian Institute of Metals*, vol. 74, no. 8, pp. 1943-1968, 2021.

[15] D. Chakradhar, and S. Narendranath, "Analysis of the effect of friction stir welding parameters on characteristics of AA6061 composites using response surface methodology," *Transactions of the Indian Institute of Metals*, vol. 74, no. 6, pp. 1303-1319, 2021.

[16] R. Mirabzadeh, V. Parvaneh, and A. Ehsani, "Experimental and numerical investigation of the generated heat in polypropylene sheet joints using friction stir welding (FSW)," *International Journal of Material Forming*, vol. 14, no. 5, pp. 1067-1083, 2021.

[17] M. Ahmadnia, S. Shahraki, and M. A. Kamarposhti, "Experimental studies on optimized mechanical properties while dissimilar joining AA6061 and AA5010 in a friction stir welding process," *The International Journal of Advanced Manufacturing Technology*, vol. 87, no. 5, pp. 2337-2352, 2016.

[18] G. Yu, X.Chen, B. Zhang, K. Pan, and L. Yang, "Tensile-shear mechanical behaviors of friction stir spot weld and adhesive hybrid joint : Experimental and numerical study," *Metals*, vol. 10, no. 8, pp. 1028, 2020.

[19] S. Prasomthong, and S.Charoenrat, "The optimization of welding hardfacing on wear resistance of FC-25 grey cast iron steel substrate by response surface methodology (RSM)," *SNRU Journal of Science and Technology*, vol. 14, no. 2, pp. 1-8, 2022

[20] S. Charoenrat, and S. Prasomthong, "Consideration of the optimizing condition in welding hardfacing on wear resistance with hot-wire gas tungsten arc welding process by response surface methodology (RSM)," *The Journal of Industrial Technology*, vol. 17, no. 2, pp. 87-102, 2021.